Available online at www.sciencedirect.com
ScienceDirect
Progress in Solid State Chemistry 35 (2007) 241–248
Progress in Solid State Chemistry
www.elsevier.com/locate/pssc

Preparation of epitaxial $La_{0.6}Ca_{0.4}Mn_{1-x}Fe_xO_3$ ($x = 0$, 0.2) thin films: Variation of the oxygen content

S. Canulescu [a], Th. Lippert [a,*], A. Wokaun [a], R. Robert [b], D. Logvinovich [b], A. Weidenkaff [b], M. Döbeli [a,c], M. Schneider [d]

[a] *Paul Scherrer Institut, OFLB/U110, 5232 Villigen, Switzerland*
[b] *EMPA Überlandstrasse 129, 8600 Duebendorf, Switzerland*
[c] *Paul Scherrer Institut, c/o ETH Hönggerberg, 8093 Zurich, Switzerland*
[d] *Laboratory for Neutron Scattering, Paul Scherrer Institut, 5232 Switzerland*

Abstract

Perovskite thin films with a nominal composition of $La_{0.6}Ca_{0.4}Mn_{1-x}Fe_xO_3$ ($x = 0$, 0.2) were deposited by pulsed reactive crossed beam laser ablation. The film properties, such as electrical conductivity and magnetoresistance are studied as a function of the oxygen content and substrate type. The oxygen content of the thin films was determined by Rutherford Backscattering and controlled by varying the background gas pressure, pressure of the gas pulse and by using alternatively O_2 and N_2O as the gas pulse.

$LaAlO_3$ and $SrTiO_3$ were used as substrates at deposition temperature of 650 °C. The grown films were analyzed by X-ray diffraction in order to optimize the growth conditions, i.e. to obtain epitaxial thin films. Thin films doped with 20% Fe were grown under the same experimental conditions as the undoped LCMO films and the effect of the doping on the structural and transport properties of the thin films has been investigated.

The temperature of the metal–insulator transition was measured as a function of the oxygen content and substrate type.

Keywords: PRCLA; Oxygen stoichiometry; Manganites

* Corresponding author. Tel.: +41 56 3104076; fax: +41 56 3102688.
E-mail address: thomas.lippert@psi.ch (Th. Lippert).

0079-6786/$ - see front matter © 2007 Published by Elsevier Ltd.
doi:10.1016/j.progsolidstchem.2007.01.023

Contents

1. Introduction

A large research effort has been devoted in recent years to manganese oxides to take advantage of their interesting properties, i.e. metal to insulator transition and colossal magnetoresistance (CMR). Doped manganites, with general formula $Ln_{1-x}Ca_xMnO_3$ (Ln = Sr, Ca, La) have been intensively studied, as they are considered as potential candidates for industrial applications [1]. Increased attention has been given to the compound $La_{1-x}Ca_xMnO_3$, where the ions La^{3+} and Ca^{2+} have very similar ionic radius, e.g. 1.36 and 1.38 Å respectively. The Ca doped $LaMnO_3$ manganites have mixed valence Mn^{3+}/Mn^{4+} with the configuration $(t_{2g})^3(e_{g1})^1$ for Mn^{3+} and $(t_{2g})^3$ for Mn^{4+}. By changing the ratio La/Ca and by varying the temperature, the transport properties of the $La_{1-x}Ca_xMnO_3$ materials can be tuned from insulating to metallic state [2]. The magnetic properties can vary from paramagnetic, ferromagnetic to antiferromagnetic by changing the doping in the cationic site. In the ferromagnetic region, corresponding to a doping range $0.3 < x < 0.7$, a drop in the resistivity has been observed at the transition point from metal to semiconductor followed by the colossal magnetoresistive effect (CMR). The double exchange mechanism, which is often used to explain the CMR phenomena [3], consists of an exchange of the e_g electrons between neighboring Mn ions leading to parallel alignment of the spin, e.g. ferromagnetism ordering [4]. Another mechanism has been also suggested for a qualitative explanation of the experimental data and it consists in a strong electron–phonon interaction arising from the Jahn–Teller splitting of the outer Mn d level [5]. A localized lattice distortion induced by the Jahn–Teller effect was indicated to have a significant contribution to the CMR mechanism.

The double exchange mechanism is related to the $Mn^{3+}–O^{2-}–Mn^{4+}$ bond distance and angle [6,7]. The physical properties of the manganites are determined by the doping level and by the cation radius [8]. The radius of the cationic atom influences the $Mn^{3+}–O^{2-}–Mn^{4+}$ distance and the probability of electrons' transfer between the Mn ions. In this case, the tendency of an increasing transition point temperature with an increase of the radius size was observed.

Oxygen content in the films strongly affects the transport properties of the films. Several reports in the literature showed the importance of the oxygen in the transfer mechanism of the films [9,10]. After applying an annealing treatment, LCMO films exhibit a lower resistance and a more pronounced CMR effect.

A broadening of the ferromagnetic transition and a decrease in the magnetization was reported in the case of Fe doped compounds, $La_2MnCo_{1-x}Fe_xO_6$ ($0 < x < 0.5$), as Co is gradually substituted by Fe [11]. Several structural investigations on the Fe doped perovskites showed that the LCMO structure does not cause lattice distortion of the unit cell [1,12–14].

In this paper, we study the systems $La_{0.6}Ca_{0.4}Mn_{1-x}Fe_xO_3$ ($x = 0$, 0.2) processed as thin films by the PRCLA method and the effect of the substitution of Mn by another transition metal, e.g. 20% Fe.

2. Experimental

The samples were prepared by pulsed reactive crossed beam laser ablation (PRCLA) using a KrF excimer laser ($\lambda = 248$ nm, $\nu = 10$ Hz) at a laser fluence of 7 J/cm^2. The PRCLA method involves the interaction of the laser-induced plasma with a reactive gas pulse synchronized with the laser. A more detailed description of the method is described elsewhere [15]. Two cylindrical targets with a nominal composition $La_{0.6}Ca_{0.4}Mn_{1-x}Fe_xO_3$ ($x = 0$, 0.2) were used in the deposition process and the films were grown on $LaAlO_3$ (100) and $SrTiO_3$ (100) substrates at a substrate temperature of 650 °C. The substrate heating was performed through a Si wafer in contact with the oxide substrate. The heating was performed with an average heating ramp of 8 °C/min and a fast cooling was applied after the deposition in vacuum atmosphere. The target to substrate distance was kept constant at 4 cm in all experiments. The variable parameter was the applied gas pulse, e.g. N_2O and O_2 at a gas pulse pressure of 2 bar. During the deposition process, a low background oxygen pressure of 8×10^{-2} Pa was maintained in the chamber.

The structural quality of the films was analyzed with a Siemens (D5000) diffractometer, equipped with a Eulerian cradle for texture analysis. Surface morphology of the films was investigated with Atomic Force Microscope (AFM), in contact mode on surface areas between 1 and 5 μm^2. The film composition was analyzed by Rutherford Backscattering (RBS) spectrometry and Elastic Recoil Detection Analysis (ERDA). The RBS measurements were performed using a 2 MeV ^{4}He beam and a silicon surface barrier detector at 165°. The collected RBS data were simulated using the RUMP software [16]. For the ERDA analysis a 12 MeV ^{127}I beam at an incidence angle of 18° was used. The scattered recoils were identified by the combination of a time-of-flight spectrometer with a gas ionization chamber.

The transport properties of the films were measured with a Quantum Design Physical Properties Measurement System (PPMS) in AC mode and over a temperature range of 50–300 K. Contacts were applied on the sample in a linear arrangement, using a silver paste.

3. Results and discussions

Fig. 1 shows typical XRD patterns of an iron doped LCMO films grown on $LaAlO_3$ substrates. The presence of only (100), (200) and (300) pseudocubic reflections of film and

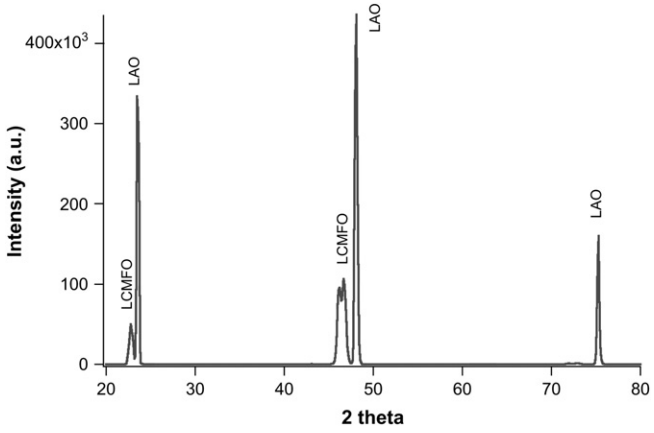

Fig. 1. XRD scans of the LCMFO films prepared on the LAO (100) substrate.

substrate reveals that the film is grown in an oriented way. All the films grown under the described experimental conditions exhibited an epitaxial growth, independent of the substrate used in the deposition process (LAO (100) or STO (100)). The films have a slightly distorted pseudocubic crystallographic structure. The lattice parameters of the pseudocubic unit cell are described by the relations $a_{pc} \approx a \approx b \approx c$. The lattice parameters calculated from XRD data are 3.890 Å for LCMFO and 3.897 Å for LCMO. The lattice parameters of the LAO (100) and STO (100) substrates with cubic structure are $a = 3.79078$ Å and $a = 3.9012$ Å, respectively.

The lattice mismatch α along the interface, defined as $\alpha = (a_{p\ substrate} - a_{p\ bulk})/a_{p\ substrate}$, gives the following values for the substrates used: $\alpha_{LAO} \approx -0.026\%$, $\alpha_{STO} \approx 0.0003\%$.

XRD investigations performed on the LCMFO samples showed that Fe is distributed in the manganate structure without inducing significant structural changes in the crystalline structure due to the almost identical ionic radius. Similar results have been reported in the earlier studies [17].

The surface morphology measurements were done in contact mode of the AFM. The scans showed low roughness and all the measurements have been performed over an area of maximum $5 \times 5\ \mu m^2$ in order to obtain detailed information about the topography. In our experiments, O_2 and N_2O gas pulses were applied in low oxygen pressure (8×10^{-2} Pa) during the deposition. Fig. 2a and Fig. 2b show the scan area for the LCMO/LAO films deposited with N_2O and O_2, respectively, as a gas pulse. For the films grown with N_2O as gas pulse, the surface morphology can be described by round grain sizes of equal dimensions and with a uniform distribution on the surface. In the case of the O_2 gas pulse, an increase of the grain size with small agglomerations on the surface was observed. As a consequence, due to the surface agglomerations, the calculated RMS values are higher for O_2 in comparison with N_2O (see Fig. 2a and b). Similar investigations reported earlier on the perovskite compounds like $La_{0.7}Ca_{0.3}CoO_3$ showed that the particle size and type of morphology can be influenced by varying the oxidizing source [15].

The same preparation procedure with different oxidizing gases was applied on the LCMFO films (see Fig. 3a and b). The surface topography of the films is significantly different than in the undoped samples with lower roughness, e.g. RMS = 6 Å for the O_2 and RMS = 9 Å for N_2O.

A higher oxygen content in the films is a crucial factor which affects the ferromagnetic transition and gives rise to a shifting of the metal–insulator transition to higher temperatures

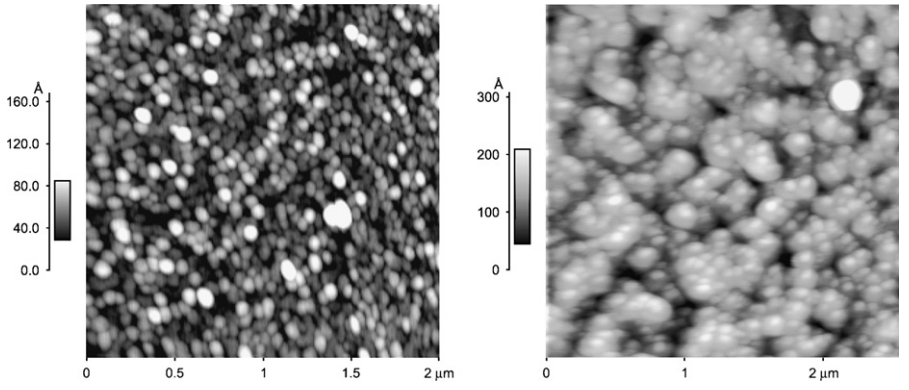

Fig. 2. AFM images of the LCMO/LAO films grown at 2 bar N_2O (a) and 2 bar O_2 gas pulse (b). The roughness values calculated were RMS = 16 Å and RMS = 30 Å.

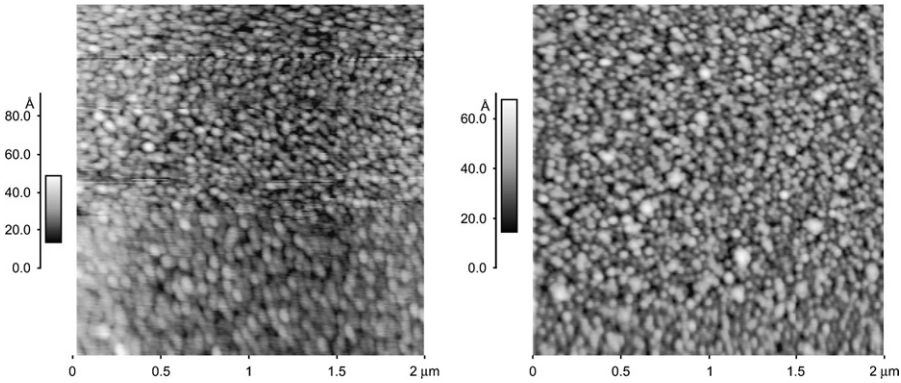

Fig. 3. Surface morphology investigations of the LCMFO/LAO thin films deposited with N_2O gas pulse (left) and O_2 gas pulse (right) AFM studies. The average grain size is around 50 nm for both samples.

[18,19]. Therefore, RBS measurements performed on the films LCMO and LCMFO showed a congruent transfer of the material. The results are summarized in Table 1.

During the RBS measurements experimental problems have been encountered which result in a high uncertainty of the quantitative oxygen and content for samples (c) and (d). It is therefore only possible to compare the stoichiometry of samples (c) and (d) directly, but a comparison between (b), (a), (d) and (c) is not possible.

Comparing the stoichiometry of the samples (a) and (b), deposited in the same experimental conditions, undoped and doped with Fe, the oxygen content in the films was found to be the same (see Table 1). We can conclude that the Fe^{3+} ion substitutes the Mn in the perovskite structure, without affecting the oxygen content. The ratio La/Ca shows a small difference, with errors of 10% in the measurements.

It is worth to point out that RBS yields an overall composition of the oxygen content in the films. The sample might contain also secondary phases that are not detected by XRD, which revealed a perovskite structure of the films, e.g. an oxygen stoichiometry close to 3.

Comparing the samples (c) and (d) deposited with O_2 and N_2O, respectively, as a gas pulse, it can be seen that the ratio of the oxygen is much higher in the second case.

As it has been suggested before [20], when the N_2O gas pulse is used, a higher amount of oxygen atoms are present due to the more facile dissociation of N_2O in comparison with O_2, resulting in films with higher oxygen stoichiometry. Emission spectroscopy studies performed on the target $La_{0.67}Sr_{0.33}MnO_3$ [21] have shown that the emission intensity from MnO is one order of magnitude higher for N_2O than for O_2, so the probability of forming gas-phase MnO during the ablation of manganites increases when N_2O is used as gas pulse. Our results

Table 1
Stoichiometry evaluation of the $La_{0.6}Ca_{0.4}Mn_{1-x}Fe_xO_3$ ($x = 0$, 0.2) films

Target material	Films' composition	Gas pulse
(a) $La_{0.6}Ca_{0.4}MnO_3$	$La_{0.72\pm0.036}Ca_{0.28\pm0.014}Mn_{0.85\pm0.0425}O_{2.5\pm0.12}$	2 bar $O_2 + O_2$ background
(b) $La_{0.6}Ca_{0.4}Mn_{0.8}Fe_{0.2}O_3$	$La_{0.8\pm0.08}Ca_{0.2\pm0.02}Fe_{0.2\pm0.05}Mn_{0.8\pm0.05}O_{2.5\pm0.15}$	2 bar $O_2 + O_2$ background
(c) $La_{0.6}Ca_{0.4}Mn_{0.8}Fe_{0.2}O_3$	$La_{0.6\pm0.06}Ca_{0.27\pm0.02}Fe_{0.2\pm0.05}Mn_{0.82\pm0.05}O_{2.1\pm0.15}$	2 bar $O_2 + O_2$ background
(d) $La_{0.6}Ca_{0.4}Mn_{0.8}Fe_{0.2}O_3$	$La_{0.6\pm0.06}Ca_{0.25\pm0.02}Fe_{0.2\pm0.05}Mn_{0.81\pm0.05}O_{2.5\pm0.15}$	2 bar $N_2O + O_2$ background

are in agreement with previous investigations and an increase of the oxygen content is observed for the more reactive gas, e.g. N_2O.

We further discuss the transport properties of the films deposited using the two different gases synchronized with the pulsed laser. The effect of oxygen incorporation in the manganite compounds like $La_{1-x}Ca_xMnO_3$ has been widely studied in the last period [21,22]. Previous reports on oxygen deficient manganites show that the oxygen deficiency increases the resistivity and magnetoresistance. We have studied the transport properties of the LCMO/LAO films deposited by PRCLA method with O_2 as a gas pulse (not shown here). The resistance versus temperature dependence showed a metal–semiconductor transition at a temperature of 186 K. When applying a magnetic field, the resistivity decreases dramatically. A negative colossal magnetoresistance [23], defined by formula [$CMR = \rho(H) - \rho(0)/\rho(H)$] of −400% being obtained at 5 T magnetic field. As the LCMO compounds have been widely studied, we will not refer to them in this paper.

In Fig. 4a and b we present the electrical characteristics of the Fe doped LCMO thin films as function of temperature, deposited with the two different oxidizing gases. As the films' thickness was not measured, arbitrary units are indicated.

From the RBS measurements reported above, the oxygen content in the films increases when a N_2O gas pulse is applied. Both LCMFO samples show a metal to insulator transition, the transition temperature is 155 K for LCMFO films grown in O_2 atmosphere and 133 K for N_2O.

It is worth pointing out that the ferromagnetic ordering occurs due to electron exchange between neighboring Mn centers bridged by oxygen Mn^{3+}–O^2–Mn^{4+}.

The Mn^{3+}/Mn^{4+} ratio can be modified by changing the oxygen content in the films [10], in such a way that the higher oxygen content induces a higher amount of Mn^{4+} ions. Fe is found invariably in the valence state 3+, and a direct substitution of Mn^{3+} by Fe^{3+} occurs [1]. Each Fe^{3+} ion that substitutes a Mn^{3+} ion will perturb the long order ferromagnetic interaction, weakening the double exchange mechanism [24], and the interaction between Mn^{4+} (d^3) ions and Fe^{3+}(d^5) leads to an antiferromagnetic coupling.

In the doped compounds $La_{0.6}Ca_{0.4}Mn_{1-x}Fe_xO_{3-\delta}$ a decrease in the mobility is confirmed by the theoretical model due to the presence of Fe in the network Fe^{3+}–O^2–Mn^{4+} [24].

A similar order of magnitude of the resistance (10^6 Ω) has been obtained for the LCMFO/STO films but an increase of T_{MI} by 6 K was obtained when LAO substrate were used instead of STO. This might be due to the slightly larger lattice mismatch between the film and the

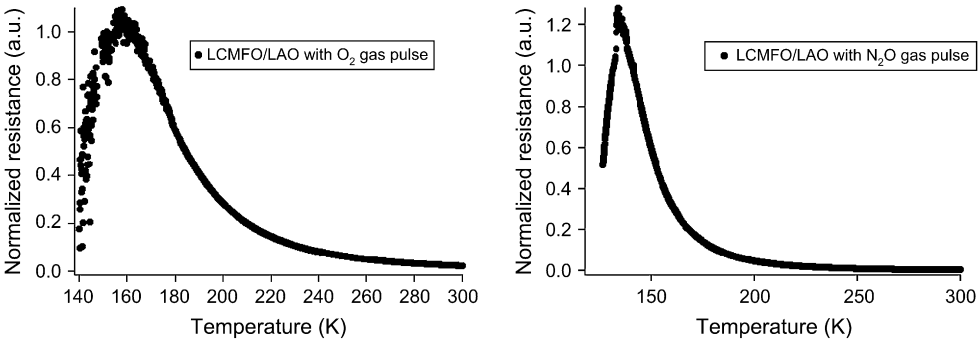

Fig. 4. Resistance versus temperature dependence for the LCMFO/LAO thin films deposited at 2 bar gas pulse pressure. (a) Corresponds to the films deposited with O_2 and (b) to the films grown in the presence of N_2O gas pulse.

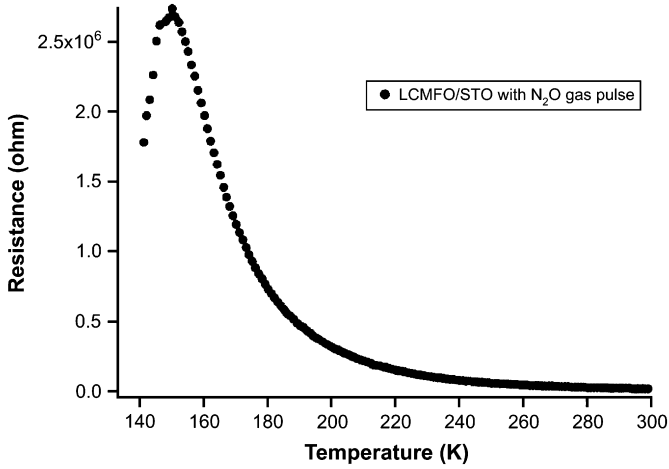

Fig. 5. Temperature dependence on the electrical resistance on the films $La_{0.6}Ca_{0.4}Mn_{0.8}Fe_{0.2}O_{3-\delta}$ grown on $SrTiO_3$ (100) at 2 bar N_2O.

substrate in the case of LAO. The larger mismatch between the film and LAO substrate involves a compression of the unit cell in an out of plane direction, the growth direction. This leads to a reduction of the Mn–O–Mn angle and an increase of the electron hopping transfer integral. As a consequence, the transition temperature increases due to the charge localization [25] (Fig. 5).

In summary, the effect of oxygen content on structural, morphological and transport properties of the $La_{0.6}Ca_{0.4}Mn_{1-x}Fe_xO_3$ ($x = 0$, 0.2) films have been studied. Similar ionic radius for Mn and Fe give the possibility of Mn substitution by Fe in the perovskite structure without significant structural modifications. The films have been grown by the PRCLA method using O_2 and N_2O pulsed synchronized gases during the deposition. Low surface roughness has been obtained in both cases and from RBS measurements it was found that the N_2O increases the oxygen content in the films. The temperature of the transition, T_{MI}, for the samples with low oxygen content is 20 K higher than that for the samples with higher oxygen content. The introduction of Fe 20% in the Mn sites leads to an increase of resistivity.

Acknowledgments

The authors are grateful to Dr Donagh O'Mahony for the English revisions and thank Paul Scherrer Institut for financial support.

References

[1] Ahn KH, Wu XW, Liu K, Chien CL. Phys Rev B 1996;54:15299.
[2] Ziese M, Semmelhack HC, Han KH, Sena SP, Blythe HJ. J Appl Phys 2002;91:9930.
[3] Zener C. Phys Rev 1951;82:403.
[4] Vengalis B, Maneikis A, Anisimovas F, Butkute R, Dapkus L, Kindurys A. J Magn Mag Mater 2000;211:35.
[5] Millis AJ, Littlewood PB, Shraiman BI. Phys Rev Lett 1995;74:5144.
[6] Anderson PW, Hasegawa H. Phys Rev 1955;100:675.

[7] Hwang HY, Cheong SW, Radaelli PG, Marezio M, Batlogg B. Phys Rev Lett 1995;75:914.
[8] Malavasi L, Ritter C, Mozzati MC, Tealdi C, Saiful Islam M, Bruno Azzoni C, Flor G. J Solid State Chem 2005;178:2042.
[9] Hsu LS, Liu CJ, Wu TW, Luca D. J Optoelectron Adv Mater 2003;5:409.
[10] Osthover C, Schmidt K, Arons RR. Mater Sci Eng B 1998;56:164.
[11] Joseph Joly VL, Bhame SD, Joy PA, Date SK. J Magn Magn Mater 2003;261:433.
[12] Pissas M, Kallias G, Devlin E, Simopoulos A, Niarchos D. J Appl Phys 1997;81:5770.
[13] Sun JR, Rao GH, Shen BG, Wong HK. Appl Phys Lett 1998;73:2998.
[14] Shannon R. Acta Crystallographica Section A 1976;32:751.
[15] Montenegro MJ, Döbeli M, Lippert T, Muller S, Weidenkaff A, Willmott PR, et al. Thin Solid Films 2004;453-454:182.
[16] Doolittle LR. Nucl Instr Meth 1986;B15:227.
[17] Cai JW, Wang CH, Shen BG, Zhao JG, Zhan WS. Appl Phys Lett 1997;71:1727.
[18] Daoudi K, Tsuchiya T, Yamaguchi I, Manabe T, Mizuta S, Kumagai T. Appl Surf Sci 2005;247:89.
[19] Zhang W, Boyd W, Elliot M, Herrenden-Harkerand W. Appl Phys Lett 1996;69:3929.
[20] Lecoeur P, Gupta A, Duncombe PR, Gong GQ, Xiao G. J Appl Phys 1996;80:513.
[21] De Santis A, Barucca G, Bobba F, Caciuffo R, Frohlich K, Pripko M, et al. J Magn Magn Mater 2004;272-276:E1501.
[22] Mahesh R, Itoh M. Solid State Ionics 1998;108:201.
[23] Li J, Liu JM, Li HP, Fang HC, Ong CK. J Magn Magn Mater 1999;202:285.
[24] Tzavellas A, Trohidou KN, Kechrakos D, Moutis N. Appl Phys Lett 2000;77:3627.
[25] Lu CJ, Wang ZL, Kwon C, Jia QX. J Appl Phys 2000;88:4032.